Chemical Vapor Deposition of Gallium Sulfide: Phase Control by Molecular Design

Andrew N. MacInnes,† Michael B. Power,† and Andrew R. Barron*

Department of Chemistry, Harvard University, Cambridge, Massachusetts 02138

Received April 30, 1993. Revised Manuscript Received July 8, 1993®

Gallium sulfide (GaS) thin films have been grown at 380–420 °C by atmospheric pressure metal–organic chemical vapor deposition (MOCVD) using the single-source precursors $[(^tBu)_2Ga(S^tBu)]_2$, $[(^tBu)GaS]_4$, and $[(^tBu)GaS]_7$. Characterization of the films by X-ray photoelectron spectroscopy (XPS), Rutherford backscattering (RBS), and energy-dispersive X-ray (EDX) analysis shows all the films to be of chemical composition Ga:S (1:1). However, from transmission electron microscopy (TEM) and X-ray diffraction (XRD) the film structure was found to be dependent on the molecular precursor. In the case of films grown from $[(^tBu)_2Ga(S^tBu)]_2$ deposition results in the formation of the thermodynamic hexagonal phase of GaS. Deposition using $[(^tBu)GaS]_4$ as the precursor gives a novel metastable face-centered cubic phase of GaS. Use of $[(^tBu)GaS]_7$ as the precursor results in amorphous films. The relationship between the molecular precursor and the deposited films is discussed in terms of the possibility of molecular control over solid-state phase synthesis.

Introduction

"Form follows function" is an axiom traditionally applied to the ergonomic design of consumer goods in the macroscopic world. It has become chic, however, to apply this concept to the microscopic world. In particular, many workers have recently expounded the idea of "molecules to materials", in which molecular species are converted, by either thermal or photochemical decomposition, to simple inorganic materials such as oxides, carbides, phosphides, etc. The vast majority of chemical studies have employed molecules which contain all the elements required in the final material, hence the term "single-source precursor", and have often consisted of a molecular structure related (in part) to the structure of required phase. Thus, in the earliest studies, for a material ME, precursors with M–E bonds were investigated.[1] More recently, researchers have synthesized molecules with core structures designed to mimic a fragment of the target solid-state phase. While this concept has led to the elegant synthesis of known materials,[2] especially in the field of III–V semiconductor compounds,[3] it is only recently that previously unreported (or unstable) phases (and materials) have been prepared. The groups of Gladfelter[4] and Wolczanski[5] have reported the formation of cubic GaN and cubic TaN respectively, by the solid-state pyrolysis of molecular precursors whose metal–nitrogen cores are subunits of the resulting solid-state phase. In a recent publication[6] we have expanded these results to the vapor phase. The metal–organic chemical vapor deposition (MOCVD) of InS using the dimeric indium thiolate precursor $[(^tBu)_2In(S^tBu)]_2$ does not yield the thermodynamic orthorhombic phase but rather the metastable high-pressure tetragonal phase.[6] This result prompted us to further study the possibility of controlling the deposited phase by the molecular design of the precursor. Our recent studies of the chemistry of gallium thiolate and sulfide compounds[7-9] provided us with a sequence of possible precursor compounds with distinctive structures.

In a preliminary communication,[10] we reported the MOCVD of a new cubic phase of GaS using the cubane precursor $[(^tBu)GaS]_4$. We now describe full details of the MOCVD of GaS thin films from three structurally distinct precursors, dimeric $[(^tBu)_2Ga(S^tBu)]_2$, tetrameric $[(^tBu)GaS]_4$, and heptameric $[(^tBu)GaS]_7$ and discuss the control they exert on the structure of the resulting films.

Results and Discussion

The majority of previous work on single-source precursors has been related to the growth of III–V semiconductor materials and has concentrated on the dimeric and trimeric pnictides **I** and **II**.[11]

It is unsurprising, therefore, that in the area of group III–chalcogenide CVD, analogous thiolate[6,12,13] and sele-

† Present address: Gallia, Inc., Weston, MA 02193.

* To whom correspondence should be addressed.

® Abstract published in *Advance ACS Abstracts*, August 15, 1993.

(1) For recent review articles see: (a) Bradley, D. C. *Chem. Rev.* **1989**, *89*, 1317. (b) Girolami, G. S.; Gozum, J. E. *Mater. Res. Soc., Symp. Proc.* **1990**, *168*, 319.

(2) See for example: (a) Interrante, L. V.; Sigel, G.; Garbauskas, M.; Hejna, C.; Slack, G. A. *Inorg. Chem.* **1989**, *28*, 252. (b) Suls, F. C.: Interrante, L. V.; Jiang, Z. *Inorg. Chem.* **1990**, *29*, 2899.

(3) See for example, Cowley, A. H.; Harris, P. R.; Jones, R. A.; Nunn, C. M. *Organometallics* **1991**, *10*, 652.

(4) Hwang, J.-W.; Hanson, S. A.; Britton, D.; Evans, J. F.; Jensen, K. F.; Gladfelter, W. L. *Chem. Mater.* **1990**, *2*, 342.

(5) Banaszak Holl, M. M.; Wolczanski, P. T.; VanDuyne, G. D. *J. Am. Chem. Soc.* **1990**, *112*, 7989.

(6) MacInnes, A. N.; Cleaver, W. M.; Barron, A. R.; Power, M. B.; Hepp, A. F. *Adv. Mater. Opt. Electron.* **1992**, *1*, 229.

(7) Power, M. B.; Barron, A. R. *J. Chem. Soc., Chem. Commun.* **1991**, 1315.

(8) Power, M. B.; Ziller, J. W.; Tyler, A. N.; Barron, A. R. *Organometallics* **1992**, *11*, 1055.

(9) Power, M. B.; Ziller, J. W.; Barron, A. R. *Organometallics* **1992**, *11*, 2783.

(10) MacInnes, A. N.; Power, M. B.; Barron, A. R. *Chem. Mater.* **1992**, *4*, 11.

(11) For a recent review article see: Jones, A. C. *Chemtronics*, **1989**, *4*, 15.

(12) (a) Nomura, R.; Konishi, K.; Matsuda, H. *Thin Solid Films* **1991**, *198*, 339. (b) Nomura, R.; Konishi, K.; Futenma, S.; Matsuda, H. *Appl. Organomet. Chem.* **1990**, *4*, 607. (c) Nomura, R.; Fujii, S.; Kanaya, K.; Matsuda, H. *Polyhedron* **1990**, *9*, 361.

(13) MacInnes, A. N.; Barron, A. R.; Power, M. B.; Hepp, A. F. *J. Organomet. Chem.* **1993**, *449*, 95.

0897-4756/93/2805-1344$04.00/0

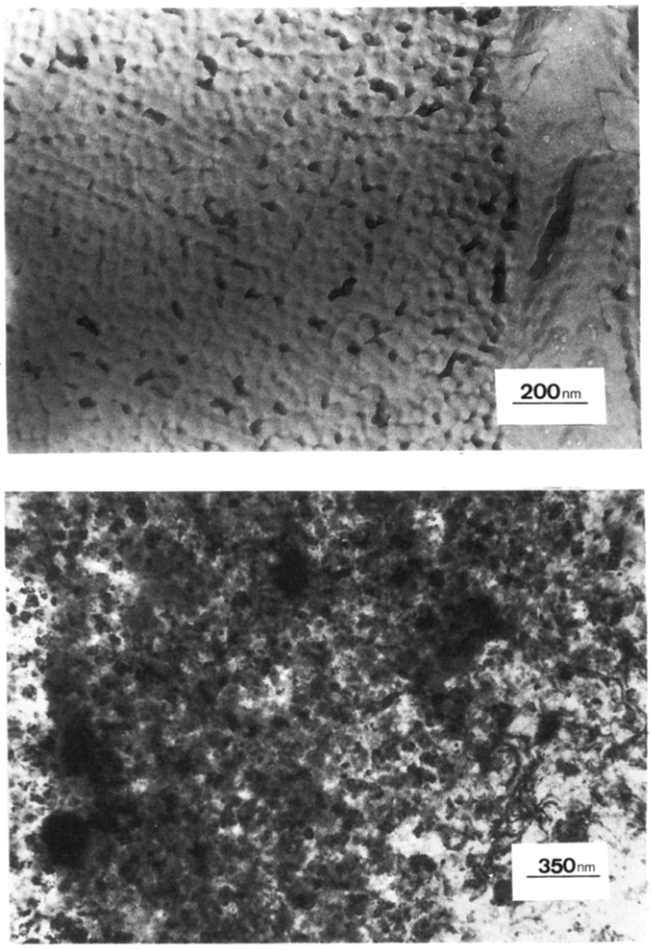

Figure 1. Bright-field TEM image of films grown from $[(^tBu)_2Ga(S^tBu)]_2$ at 400 °C before (a) and after (b) thermal annealing at 475 °C for 15 min.

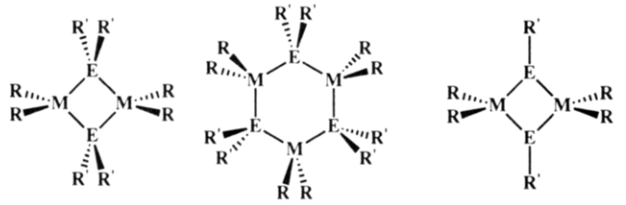

M = Al, Ga, In; E = N, P, As, Sb

(I)

(II)

M = Ga, In; E = S, Se

(III)

nolate[14] compounds **III** have been employed as single-source precursors for indium sulfide and selenide thin films, respectively. On the basis of precedent, it is reasonable to postulate that the gallium thiolate dimer $[(^tBu)_2Ga(S^tBu)]_2$ (**IV**)[8] should be a suitable precursor

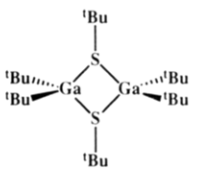

(IV)

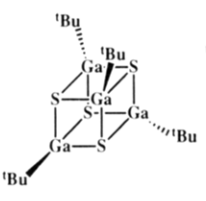

(V)

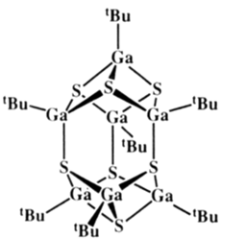

(VI)

for GaS. We have previously noted[6] that deposition using $[(^tBu)_2In(S^tBu)]_2$ below 380 °C results in the formation of sulfur-deficient films with $^tBuSS^tBu$ as a volatile coproduct and have proposed that this is due to the higher relative bond strength of the S–C bond than the In–S bond.[6] While such an effect may not be an issue for the

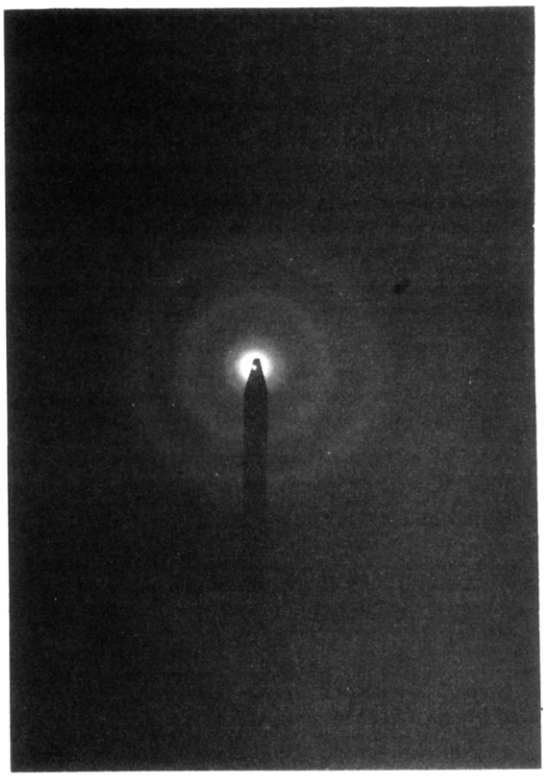

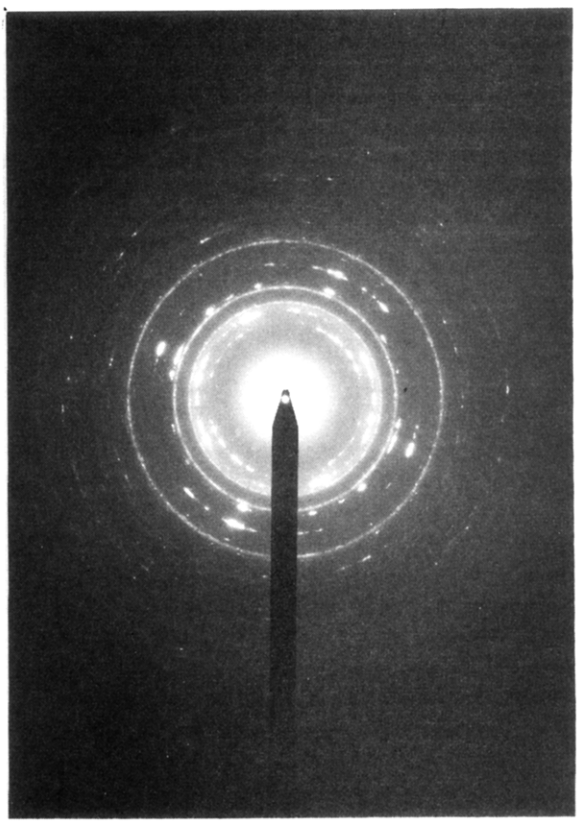

Figure 2. Selected area diffraction pattern of films from $[(^tBu)_2Ga(S^tBu)]_2$ at 400 °C before (a) and after (b) thermal annealing at 475 °C for 15 min.

(14) Gysling, H. J.; Wernberg, A. A.; Blanton, T. N. *Chem. Mater.* **1992**, *4*, 900.

Table I. Summary of the Dependence of the GaS Phase with Precursor and Deposition Temperature

precursor	deposition temp (°C)	Ga:S ratio	phase observed
$[(^t\text{Bu})_2\text{Ga}(\text{S}^t\text{Bu})]_2$	400	50:50	hexagonal GaS (poorly crystalline)
$[(^t\text{Bu})_2\text{Ga}(\text{S}^t\text{Bu})]_2$	475	40:60	amorphous
$[(^t\text{Bu})\text{GaS}]_4$	<380	50:50	amorphous
$[(^t\text{Bu})\text{GaS}]_4$	380–400	50:50	cubic GaS
$[(^t\text{Bu})\text{GaS}]_4$	>400	<20%, 40:60[a]	amorphous, crystalline needles[a]
$[(^t\text{Bu})\text{GaS}]_7$	380–400	50:50	amorphous

[a] Two distinct growth regions; see text for details.

gallium analog, we decided to investigate precursors in which no S–C bonds are present. Additionally, if we wish to determine whether the molecular structure of the precursor determines the phase of the deposited film, it would then be desirable to have precursors with different symmetry core structures. With regard to a core structure of higher symmetry than the Ga_2S_2 (C_{2v}) core of $[(^t\text{Bu})_2\text{Ga}(\text{S}^t\text{Bu})]_2$, we have recently reported the synthesis and crystallographic characterization of the first III–VI cubane compound $[(^t\text{Bu})\text{GaS}]_4$ (**V**).[7,8] The mass spectrum of $[(^t\text{Bu})\text{GaS}]_4$ indicates that no significant fragmentation of the Ga_4S_4 cubane occurs during complete loss of the organic substituents, and thus the highly symmetrical Ga_4S_4 core of $[(^t\text{Bu})\text{GaS}]_4$ should provide a template for a high-symmetry solid-state phase. In a similar manner the lack of any but C_3 symmetry of the related heptamer $[(^t\text{Bu})\text{GaS}]_7$ (**VI**)[9] should, if the core is retained during deposition, result in an amorphous film. While all these precursors ought to form films of the composition GaS, the diversity of symmetry in the structural motifs should, if the molecular cores are retained, provide a convenient method of controlling the solid-state structure.

Thermogravimetric analyses (TGA) of $[(^t\text{Bu})_2\text{Ga}(\text{S}^t\text{Bu})]_2$, $[(^t\text{Bu})\text{GaS}]_4$, and $[(^t\text{Bu})\text{GaS}]_7$ were performed under an inert (dry argon) atmosphere in order to determine the volatilization–decomposition window. Compounds $[(^t\text{Bu})_2\text{Ga}(\text{S}^t\text{Bu})]_2$ and $[(^t\text{Bu})\text{GaS}]_7$ sublime with some decomposition at 240 and 280 °C, respectively. In contrast, $[(^t\text{Bu})\text{GaS}]_4$ sublimes completely at 250 °C. Given the above, the following volatilization temperatures were employed for the precursors: 225 °C for $[(^t\text{Bu})_2\text{Ga}(\text{S}^t\text{Bu})]_2$ and $[(^t\text{Bu})\text{GaS}]_4$ and 240 °C for $[(^t\text{Bu})\text{GaS}]_7$.

Thin film growth was carried out on single crystal KBr, n- and p-type GaAs (100), and fused silica glass substrates in a resistively heated horizontal laminar flow glass MOCVD system operated at atmospheric pressure as previously described.[15] Purified argon was used as a carrier gas. All the coatings adhered well to all substrates (Scotch tape test). The films were all contiguous and featureless by SEM and showed uniform coverage. No appreciable difference in the gross morphology of the film as a function of substrate was noted. However, the microstructure was found to be highly dependent on the identity of the precursor and, in the case of $[(^t\text{Bu})\text{GaS}]_4$, the deposition temperature. This relationship is summarized in Table I and detailed below for each of the precursor systems.

$[(^t\text{Bu})_2\text{Ga}(\text{S}^t\text{Bu})]_2$. Films grown using the dimeric gallium thiolate $[(^t\text{Bu})_2\text{Ga}(\text{S}^t\text{Bu})]_2$ as the precursor was deposited at 400 °C. While the SEM of a film obtained from $[(^t\text{Bu})_2\text{Ga}(\mu\text{-S}^t\text{Bu})]_2$, shows the film to be smooth and featureless, the higher resolution bright-field TEM image (Figure 1a) shows a fine structure consisting of near spherical particles of about 300 Å in diameter. The associated electron diffraction (Figure 2a) displayed broad diffuse rings indicative of a very poorly crystallized film. The estimated centers of these rings gave d spacings consistent with the most intense reflections for the thermodynamically stable hexagonal ($P6_3/mmc$) phase of GaS.[16] EDX analysis indicated a film composition of Ga:S = 50:50 (±2%), in support of this identification. XPS analysis shows the film to be absent of carbon and oxygen, except for adventitious material present on the surface.

Thermal annealing (15 min at 475 °C, in a sealed tube under argon) of a TEM specimen of the as-deposited film resulted in crystallization of the film, as indicated by a significant change in the film morphology (Figure 1b) and the sharpening of the rings in the selected area electron diffraction pattern (Figure 2b). As can be seen from Table II the electron diffraction after annealing is now consistent with hexagonal GaS.[16]

Given the above result, films were deposited using $[(^t\text{Bu})_2\text{Ga}(\text{S}^t\text{Bu})]_2$ at 475 °C, in an effort to obtain crystalline films without the post deposition anneal. However, the deposited films yielded amorphous patterns and had a Ga:S ratio of 40:60 (±3%) (i.e., consistent with Ga_2S_3). This result suggests that the precursor molecule undergoes premature decomposition at 475 °C, resulting in the rupture of the Ga_2S_2 core.

$[(^t\text{Bu})\text{GaS}]_4$. X-ray photoelectron spectroscopy (XPS) analysis of films grown from $[(^t\text{Bu})\text{GaS}]_4$ at 390 ± 10 °C shows the absence of detectable carbon and oxygen beneath the surface coverage of Ga_2O_3 (see Figure 3), and are GaS (50:50 ± 2) in composition. The GaS composition was confirmed by RBS for films deposited both on GaAs and silica (e.g., Figure 4) and EDX analysis of free-standing films.

As we have previously communicated,[10] films grown on KBr plates were polycrystalline and gave an electron diffraction consistent with a face centered cubic lattice with a lattice parameter a = 5.4 Å (see Table III). Further studies on these deposited films have shown that this cubic structure shows significant expansion on thermal annealing (15 min at 450 °C) giving a measured lattice parameter for a free-standing film of 5.5 Å (Table III). Upon further annealing at higher temperatures (>500 °C) the films show signs of partial decomposition yielding a cubic phase with a reduced lattice parameter and an undefined phase, see below.[17]

By contrast with the free-standing films, those grown on GaAs (100) are not polycrystalline but near-epitaxial. This is as may be expected since the lattice parameter of the annealed GaS is within 3% of GaAs [5.653 25(2) Å].[18] Figure 5 shows the X-ray diffraction pattern of a typical

(15) Landry, C. C.; Cheatham, L. K.; MacInnes, A. N.; Barron, A. R. *Adv. Mater. Opt. Electron.* **1992**, *1*, 3.

(16) JCPDS No. 30-576.

(17) While films heated above 550 °C show a distinct diffraction pattern, it could not be matched to any known gallium sulfide (or oxide) phase.

(18) Sze, S. M. *Semiconductor Devices, Physics and Technology*; John Wiley and Sons: Chichester, 1985.

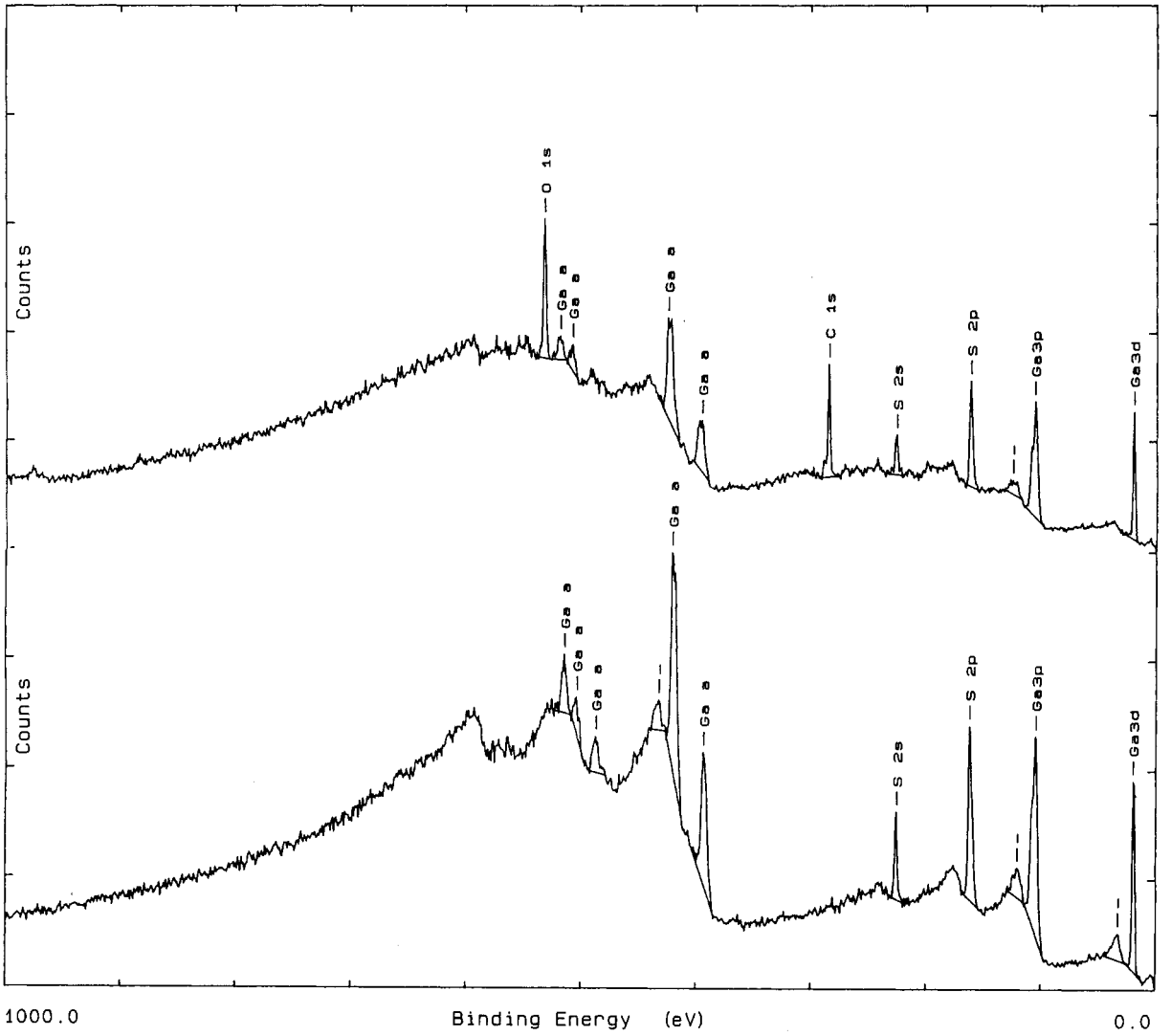

Figure 3. X-ray photoelectron spectra of GaS film grown from $[(^t\text{Bu})\text{GaS}]_4$ at 390 °C before (a) and after (b) argon ion etching.

Table II. Comparison of *d* Spacing (Å) of Hexagonal GaS with That Formed by CVD Using $[(^t\text{Bu})_2\text{Ga}(\text{S}^t\text{Bu})]_2$ as a Single-Source Precursor

hkl	I/I_0	hexagonal GaS (3-576) ($P6_3/mmc$)	as deposited *d*, Å	postanneal *d*, Å
002	93	7.742	8.0[a]	*b*
004	76	3.870		
100	100	3.106	3.1[a]	*b*
101	85	3.046		3.03
102	12	2.882		2.93
103	48	2.662		2.65
006	13	2.582		
104	26	2.423		2.46
105	52	2.193		2.13
106	8	1.985		2.03
008	3	1.937		
107	90	1.803	1.80[a]	1.83
110	72	1.794		
112	9	1.747		1.75
118	3	1.644		
200	9	1.553		1.56
201	10	1.543		
202	1	1.523		
203	6	1.487		1.50
116	11	1.473		1.47

[a] Broad rings. [b] High *d* spacing are obscured by amorphous halo.

GaS-coated GaAs (100) substrate. Two prominent peaks corresponding to *d* spacings of 2.803 and 1.409 Å are evident. Although the underlying single-crystal GaAs would allow for reflections in the regions {200} and {400}

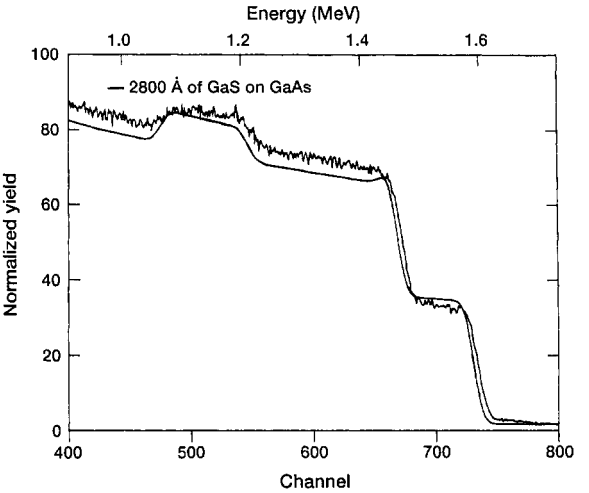

Figure 4. Rtherford backscattering spectroscopic data for GaS film grown on GaAs from $[(^t\text{Bu})\text{GaS}]_4$ at 390 °C. Data fitted using RUMP simulation for Ga:S ratio of 1:1.

at 2.828 and 1.414 Å, respectively, a higher resolution scan (Figure 6) around the {400} reflection reveals that this apparent singlet is comprised of multiple-component peaks. The small peak at 1.414 Å (marked as GaAs {400} in Figure 6) may be attributed to the substrate GaAs {400} reflection, attenuated by the GaS overlayer as expected.

Table III. Measured *d* Spacing (Å) for GaS Films Grown from [(ᵗBu)GaS]₄ Compared to Calculated Values for fcc Lattice

	as deposited, a = 5.4 Å		after thermal anneal, a = 5.5 Å	
hkl	calcd	measd	calcd	measd
111	3.10	3.11	3.18	3.19
002	2.69	2.70	2.75	2.79
022	1.90	1.83	1.94	1.88
113	1.62	1.64	1.66	1.68
222	1.55	1.56	1.59	1.59
004	1.34	1.37	1.38	1.40
133	1.23	1.22	1.26	1.27
024	1.20	1.18	1.23	1.22
422	1.10	1.08	1.12	1.11
333/511	1.04	1.06	1.06	1.06
440	0.95	0.93	0.97	0.95
531	0.91	0.90	0.93	0.93

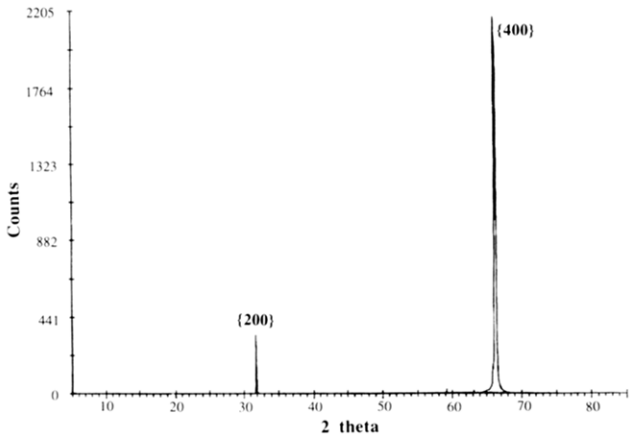

Figure 5. X-ray diffraction pattern of a typical sample of GaS, grown from [(ᵗBu)GaS]₄, deposited on GaAs (100).

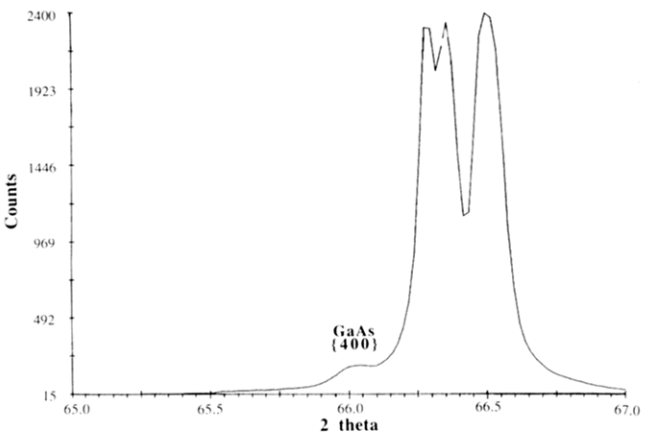

Figure 6. High resolution X-ray diffraction pattern of cubic GaS deposited on GaAs.

The other peaks are the {400} reflections of the GaS coating displaying a narrow range of *d* spacings around an average value of 1.408 Å. The origins of this range of peaks are unclear but may be the result of either strain in the growing film or the manifestation of the strained film causing curvature of the substrate and coating. The lattice parameter of this near-epitaxial GaS coating corresponds to a calculated cell constant of 5.632 Å.

Unlike the thin (<1000 Å) free-standing polycrystalline films, thermal annealing of the GaS films deposited on GaAs substrates at 550 °C for 15 min results in a change in the structure from the metastable cubic GaS phase to the thermodynamic hexagonal GaS phase. However, as can be seen from Figure 7 the GaS crystallizes with a preferred (001) orientation (*cf.*, Table II), presumably as

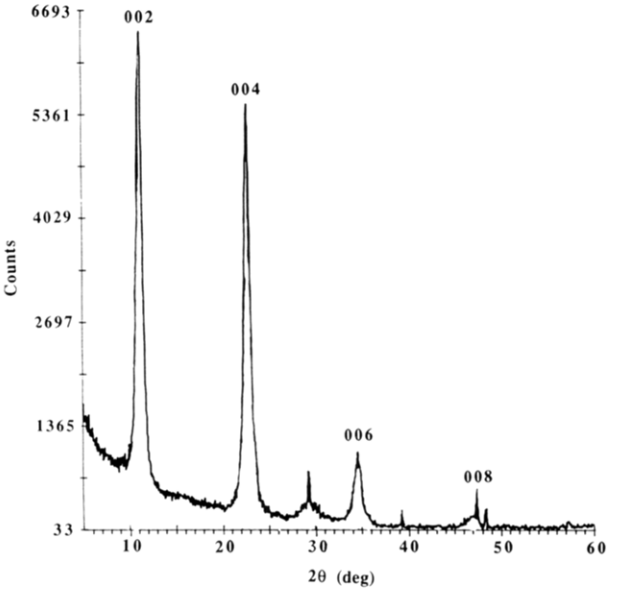

Figure 7. X-ray diffraction pattern of GaS film deposited on GaAs after annealing at 550 °C for 15 min. Hexagonal GaS peaks are indexed.

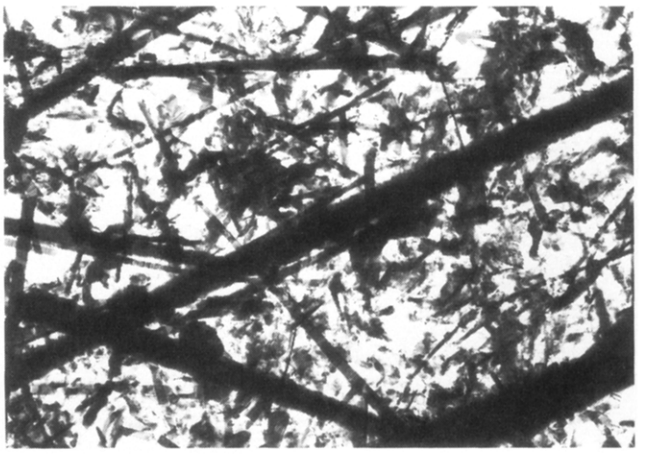

Figure 8. Bright-field TEM image of the down flow growth region of films grown from [(ᵗBu)GaS]₄ at 500 °C.

a consequence of the GaAs substrate. It is interesting to note that the GaS films deposited on GaAs substrates from either [(ᵗBu)₂Ga(SᵗBu)]₂ (above) or [(ᵗBu)GaS]₇ (below) do not crystallize under similar thermal annealing conditions.

If film deposition using [(ᵗBu)GaS]₄ is carried out above 450 °C two growth regions are observed in the chamber. The upstream deposition zone consists of an amorphous featureless gallium rich matrix containing between 0 and 20% sulfur. Down flow of this amorphous region a polycrystalline film is deposited, as indicated by the bright field TEM image (Figure 8), which shows the film to consist of fine needles on the base layer of the film. The elemental composition of the film was determined by EDX to be between GaS and Ga_2S_3. However, while the films are crystalline, the electron diffraction did not match any known gallium sulfide phase.

[(ᵗBu)GaS]₇. Films deposited from the heptamer [(ᵗBu)GaS]₇ show differences to those grown using either [(ᵗBu)GaS]₄ or [(ᵗBu)₂Ga(SᵗBu)]₂. Although over the temperatures of 390 ± 10 °C the films consist of a Ga:S ratio of 50:50 (±2), electron diffraction yielded amorphous patterns and the films are essentially featureless (Figure 9a). Thermal annealing of a TEM specimen (30 min at

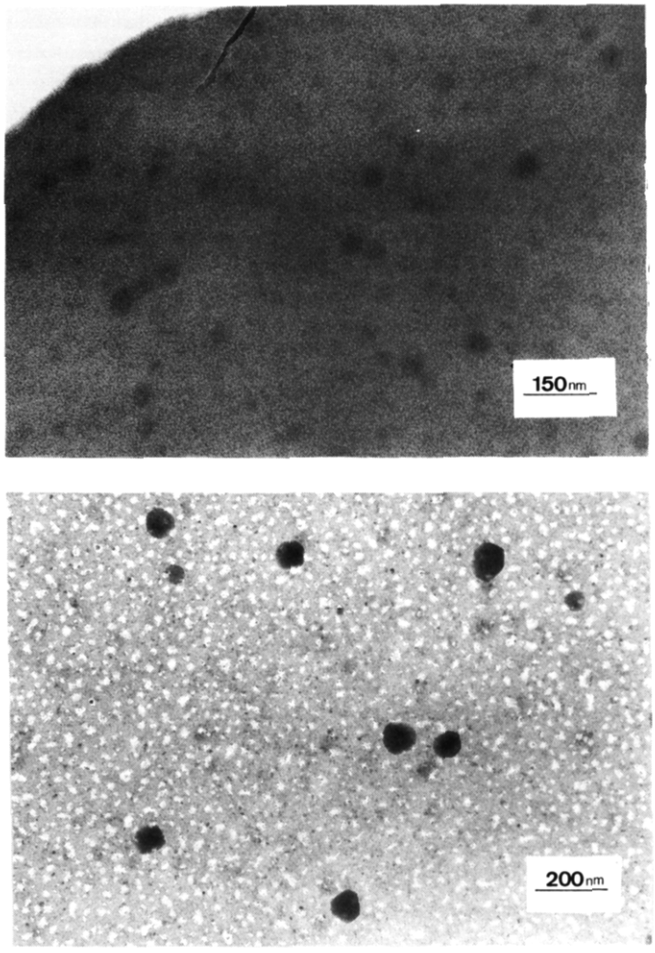

Figure 9. Bright-field TEM image of films grown from $[(^t\text{Bu})\text{GaS}]_7$, at 390 °C, before (a) and after (b) thermal annealing (30 min at 475 °C).

475 °C) resulted in its crystallization, as evident by the appearance of morphology in the film (Figure 9b), and a sharp electron diffraction pattern (Figure 10). We have, as yet, been unable to determine the identity of the crystalline phase (or phases) since it does not match GaS (hexagonal, cubic, or rhombohedral), Ga_2S_3, or Ga_2O_3. As was observed for the films grown from $[(^t\text{Bu})_2\text{Ga}(\text{S}^t\text{Bu})]_2$, films deposited from $[(^t\text{Bu})\text{GaS}]_7$ on GaAs do not crystallize upon thermal annealing.

Molecular Control over the Phase of Chemical Vapor Deposited Gallium Sulfide. Thin films of chemical composition GaS have been grown by MOCVD using three structurally distinct precursors: $[(^t\text{Bu})_2\text{Ga}(\text{S}^t\text{Bu})_2]$, $[(^t\text{Bu})\text{GaS}]_4$, and $[(^t\text{Bu})\text{GaS}]_7$. While the phase of the deposited films is clearly dependent on the identity of the precursor, it is appropriate to pose the following question: *Is the phase determined by the structure of the precursor?*

We have recently shown that the dimeric indium thiolate $[(^t\text{Bu})_2\text{In}(\text{S}^t\text{Bu})]_2$ may be used as a single-source precursor for the MOCVD of InS thin films.[6] The dimeric In_2S_2 core was proposed to account for the formation of the nonequilibrium high-pressure tetragonal phase ($I4/mmm$). While the tetragonal phase may be considered to consist of fused four-membered In_2S_2 rings (as is present in the precursor), the orthorhombic (*Pnnm*) phase consists of fused six-membered cycles in a chair conformation. Thus, while the tetragonal form may be built up from the precursor molecules' In_2S_2 core, ring rupture or rearrangement to In_3S_3 must occur for the orthorhombic form to be deposited. In the case of films deposited from $[(^t\text{Bu})_2\text{Ga}(\text{S}^t\text{Bu})]_2$, if the precursors core remains essentially intact during deposition, then the resulting phase would be expected to consist of four-membered rings, which neither of the previously known phases of GaS consist of, both consisting of a layered S–Ga–Ga–S structure built up of fused six-membered rings (e.g., Figure 11). However, if one considers the mode of packing of the 4-fold layers shown in Figure 11, it may be seen that hexagonal GaS does consist of *highly* distorted Ga_2S_2 rings; see Figure 12. While, the intralayer Ga–S distance in hexagonal GaS (2.337 Å) is similar to that expected for $[(^t\text{Bu})_2\text{Ga}(\text{S}^t\text{Bu})]_2$ (2.35–2.45 Å), the interlayer Ga···S distance is much larger (3.727 Å).[7,9] Thus, while the core of $[(^t\text{Bu})_2\text{In}(\text{S}^t\text{Bu})]_2$ is structurally matched to tetragonal InS, severe distortion of the $[(^t\text{Bu})_2\text{Ga}(\text{S}^t\text{Bu})]_2$ core is required to match hex-

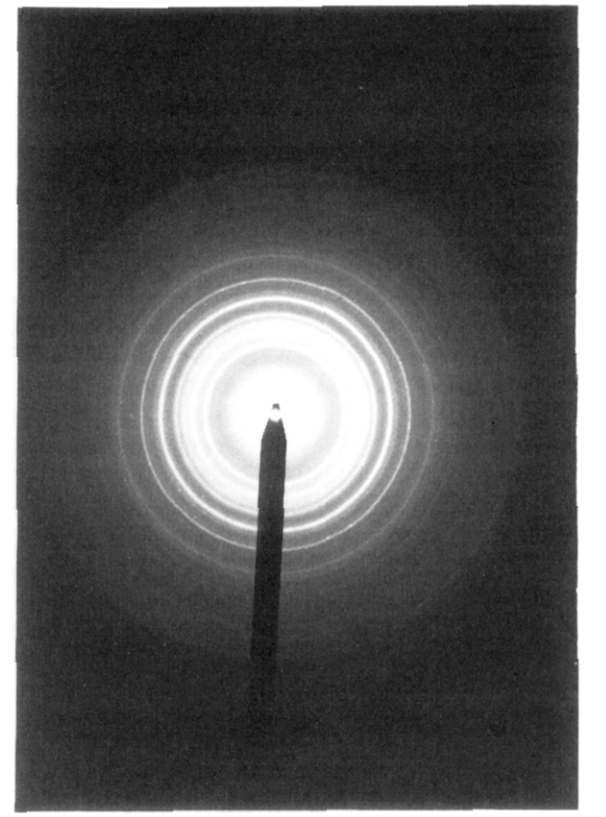

Figure 10. Electron diffraction patterns of the film grown from $[(^t\text{Bu})\text{GaS}]_7$ at 390 °C after thermal annealing (30 min at 475 °C).

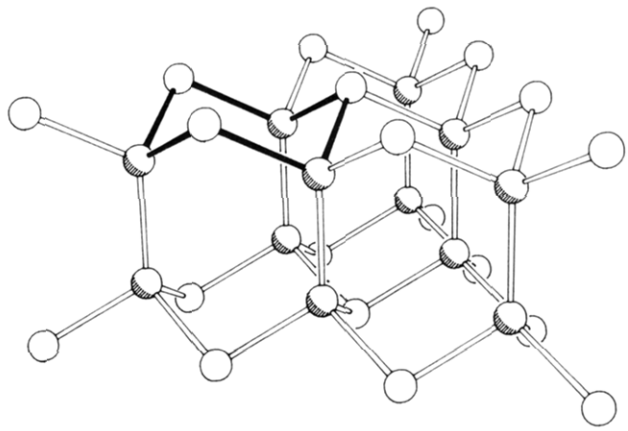

Figure 11. Unit cell structure of hexagonal GaS. The solid bonds represent the smallest cyclic structural fragment.

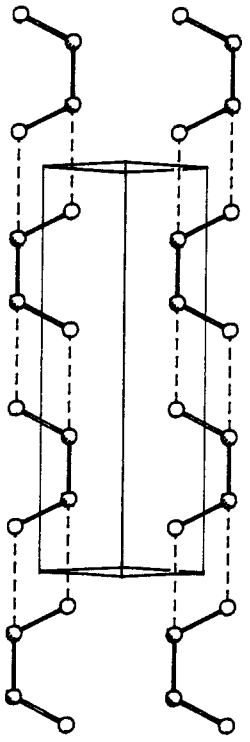

Figure 12. Interlayer stacking of hexagonal GaS viewed perpendicular to the {110} plane.

agonal GaS. As a consequence, the GaS films deposited from $[(^tBu)_2Ga(S^tBu)]_2$ are poorly crystallized, whereas the InS film grown under identical conditions are highly crystalline with strong preferred orientation. Upon thermal annealing the Ga_2S_2 dimers presumably undergo the requisite rearrangement to allow for crystallization of the hexagonal phase.

The formation of a cubic phase of GaS by the MOCVD of $[(^tBu)GaS]_4$ was previously explained in terms of the retention of the cubane precursor core in the deposited film.[19] In a simplistic view, the cubic core presumably relaxes in the deposited film and rearranges to a cubic lattice (Scheme I). The electron diffraction of the as-

Scheme I

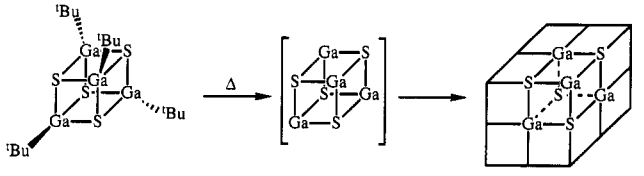

deposited films grown from $[(^tBu)GaS]_4$ is consistent with a face-centered cubic lattice.

Of the common face centered cubic structures two have a 1:1 stoichiometry; halite (NaCl) and zinc blende (cubic ZnS), which for a single compound (e.g., GaS) would have near identical diffraction patterns, the only differences being the relative intensities of certain reflections. A survey of halite and zinc blend structures of a similar cell constant to the cubic GaS, formed from $[(^tBu)GaS]_4$, show that the only consistent relative intensity between the structures is the {111} reflection is more intense than the {200} reflection for the zinc blend structure, while the {200} is more intense than the {111} for halite structures. In the electron diffraction of cubic GaS films the {111} is clearly more intense than the {200}; however, given the difficulties in quantification of electron density patterns, we originally left the nature of the exact structure open to question. Further studies lead us to the conclusion that while the films may initially grow as shown in Scheme I, cubic GaS adopts the zinc blende structure. The following evidence and observations are presented to support this conclusion:

(i) The preference of gallium for tetrahedral over octahedral coordination sites is well documented[20] and exemplified by the structure of the stable oxide phase; β-Ga_2O_3 in which the gallium is divided between tetrahedral and octahedral sites.[21] This is in comparison with alumina where all the aluminum atoms are in octahedral vacancies. A similar tetrahedral site preference to that seen for gallium is observed for iron. The tetrahedral preference for gallium should therefore favor the zinc blende structure for cubic GaS.

(ii) The cell parameter (a) for cubic-ZnS is 5.409 Å. Given the adjacent position of Ga and Zn, the cell parameter for cubic GaS would be expected to be the same or slightly larger. This is indeed observed.

(iii) If cubic GaS adopts the zinc blende structure, then the Ga–S distance calculated from the observed lattice parameters would be 2.33 and 2.38 Å for the as-deposited and thermally annealed cubic GaS, respectively, and 2.42 Å for the GaS grown on GaAs (see above). These values compare favorably to those we have previously reported for molecular gallium–sulfide (2.31–2.44 Å), and the hexagonal phase of GaS (2.337 Å).

(iv) Using the method of Mooser and Pearson,[22] which predicts the crystal structure of normal valence compounds based on the principal quantum number and electronegativities[23] of the component atoms, a zinc blende (tetrahedral coordination) structure is expected for cubic GaS.

If we assume that the cubane core of the $[(^tBu)GaS]_4$ precursor is retained during the deposition,[19] then as described in Scheme I a halite structure would ensure. However, as can be clearly be seen from Figure 13 the relationship between halite and zinc blende structure involves a simple ($^1/_4$, $^1/_4$, $^1/_4$) shift of one of the interpenetrating fcc lattices, or the movement of one element from octahedral to a tetrahedral environment. It is thus reasonable to propose that this halite to zinc blende transformation be facile on the surface of the growing film. Furthermore, during deposition on GaAs (100) the substrates surface will promote such a change. Thus, while a cubic phase is determined by the precursor, its growth is enhanced by the cubic GaAs substrate.

The use of $[(^tBu)GaS]_7$ as a single-source precursor does not allow a crystalline phase to be deposited, irrespective of substrate. If, as assumed for the dimer and tetramer and confirmed by mass spectrometric studies,[9] the core of the heptamer is not disrupted during the deposition process, it is possible to propose why no crystalline phase is produced. The Ga_7S_7 core of $[(^tBu)GaS]_7$ has a C_3 axis with no possibility of ordered close packing. Thus, during deposition a random array of gallium and sulfur atoms would be incorporated into the film. This concept is

(19) We have recently determined the gas-phase electron diffraction structure of $[(^tBu)GaS]_4$, and verified that the Ga_4S_4 cubic core remains intact in the gas phase. Hnyk, D. M.; McMurdo, G. M.; Power, M. B.; Rankin, D. W. H.; Barron, A. R., unpublished results.

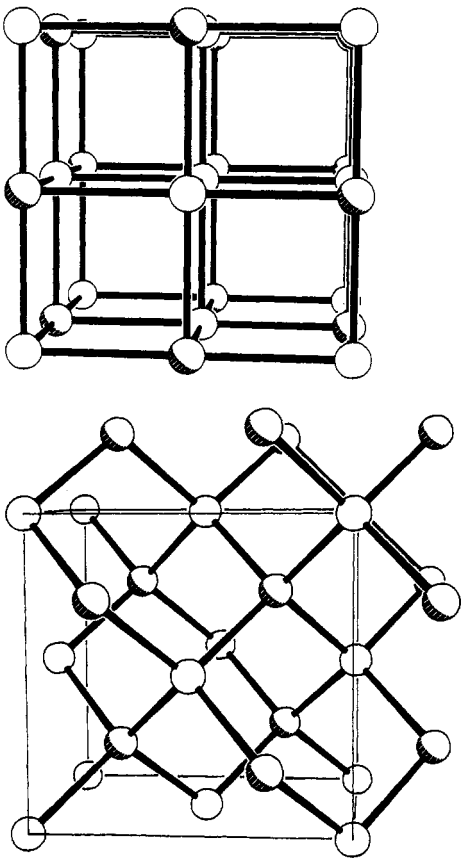

Figure 13. Structural relationship of halite (top) and zinc blende (bottom) fcc cubic structures.

consistent with the amorphous nature of the deposited films.

Experimental Section

Thermogravimetric analyses (TGA) were obtained on a Seiko 200 TG/DTA instrument using an argon carrier gas. Rutherford back-scattering (RBS) was carried out using a 2.0 MeV He^{2+} ion beam. XPS was performed on a Surface Science Instruments Spectrometer (Model SSX-100) with a monochromatized Al Kα source. The spectra were acquired with a 50-eV pass energy and a 1000-μm spot size. All samples were sputtered with 3-keV argon ions prior to data collection to remove adventitious carbon. All spectra were charge referenced independently to graphitic carbon (C_{1s} = 284.8 ± 0.1 eV) and gold (Au_{4f} = 84.0 ± 0.1 eV). TEM, and associated EDX analysis were performed on a Philips EM420 analytical electron microscope operating at 120 kV. Quantitative EDX was enabled by a Tracor-Northern analyzer and standardless metallurgical thin-film (SMTF) software program. TEM analysis of the films was enabled by the production of electron transparent (<1000 Å) films by a short duration (*ca.* 1 h) deposition onto KBr single-crystal plates. The deposited films are readily removed by immersion in deionized water; the films float off easily an may be scooped onto standard TEM grids for observation. A Rigaku RU300 and Scintag thin-film diffractometers were used for X-ray diffraction (XRD) studies. SEM studies were performed on a JEOL 6400 scanning microscope.

Unless otherwise stated, all manipulations were carried out under a nitrogen atmosphere. $[(^tBu)_2Ga(\mu\text{-}S^tBu)]_2$, $[(^tBu)GaS]_4$, and $[(^tBu)GaS]_7$ were prepared according to literature procedures.[7-9]

Chemical Vapor Deposition Studies. Depositions were carried out over a range of temperatures (380–500 °C), in an atmospheric pressure laminar-flow hot-wall glass reactor, as previously described.[15] Argon was purified using a Cr/Cr_2O_3 purifier prior to entry into the chamber. Depositions were carried out on KBr single-crystal substrates, n- and p-type (100) GaAs wafers, and fused silica glass. No appreciable difference in film morphology as a function of substrate was noted. The CVD chamber, loaded with substrates, was heated to the desired deposition temperature (see Table I) and purged with argon for about 1 h prior to deposition. The precursors were then added (*ca.* 500 mg) and brought to the desired volatilization temperature. The flow of carrier gas through the resistively heated deposition zone was between 0.5 and 1 L $min.^{-1}$ Outflow from the reaction chamber was through an oil bubbler which prevented back flow of air into the reaction chamber. Deposition times varied between 0.5 and 5 h depending on the thickness of film desired.

Acknowledgment. Financial support for this work was provided in part by the National Science Foundation and Aluminum Research Board. The National Research Council and NASA Lewis Research Center are gratefully acknowledged for a postdoctoral fellowship to M.B.P. We are indebted to John Chervinsky and David Bem for assistance with RBS and XRD measurements, respectively. We thank Dr. A. F. Hepp (NASA, Lewis), and Drs. D. J. Ciappenelli and H. W. Orf (Gallia, Inc.) for their encouragement and support of our work.

(20) See Greenwood, N. N.; Earnshaw, A. *Chemistry of the Elements*; Pergamon Press: Oxford, Great Britain, 1984; p 250.
(21) Geller, S. *J. Chem. Phys.* **1960**, *33*, 676.
(22) Mooser, E.; Pearson, W. B. *Acta Crystallogr.* **1959**, *12*, 1015.
(23) Gordy, W.; Thomas, W. J. O. *J. Chem. Phys.* **1956**, *24*, 439.